Direct Numerical Simulation and Rank Analysis of Two-Dimensional Kolmogorov-type Vortex Flows*

Mikhail A. Guzev[1] (iD) *, Alexey N. Doludenko*[2] (iD) *, Alexey D. Ermakov*[3] (iD) *,
Anna O. Posudnevskaya[3,4] (iD) *, Svetlana V. Fortova*[3] (iD)

The article is devoted to direct numerical modeling of viscous weakly compressible Kolmogorov-type flows in a square calculation cell. Several different conditions are observed. One of them is dominated by a large vortex with a well-defined average profile. In another state, strong chaotic large-scale fluctuations prevail. In the third state, laminar flow is observed. The nature of the realized state depends on the coefficient of kinematic viscosity of the liquid, the amplitude of the external pumping force, and the bottom friction coefficient. At constant values of the kinematic viscosity and the wave vector, a small value of the friction coefficient leads to the appearance of the first state. As the bottom friction coefficient increases, there is a transition from a flow with one large vortex to a laminar flow through a series of states with several unstable vortices, which we call chaotic flow. A rank analysis of the values of vorticity, energy, and pressure, as well as the frequency of their occurrence, is proposed. It is shown that for chaotic, vortex, laminar and transitional regimes of fluid motion, the inflection point in the rank frequency distributions of the above fields is a universal characteristic for classifying various types of flow.

Keywords: turbulence, numerical simulation, Kolmogorov-type flows, rank analysis.

Introduction

Two-dimensional models for describing vortex flows are widely applied in atmospheric, oceanic, and astrophysical research [19]. The applicability conditions for these models are met for processes, the horizontal scales of which are much larger than the vertical one, and it can be assumed that the main flow movement occurs in two horizontal directions. In 1959, A.N. Kolmogorov proposed to study the simplest model, which is the two-dimensional motion of a viscous fluid prompted by the action of a periodic (along one of the coordinates) field of an external force (pumping) [2]. The first theoretical works [4, 28] devoted to two-dimensional vortex structures reveal a fundamental difference in their behavior from three-dimensional ones. In the spatial case, it is known that there is a direct cascade of energy [23], which, due to nonlinear interaction, transfers energy from the integral scale, on which energy is pumped, to smaller scales up to the dissipative one, determined by viscosity, on which kinetic energy is converted into heat. In the planar case, the situation is the opposite: a reverse energy cascade occurs, in which energy is transferred from small scales to larger ones. Quantitatively, this is manifested in the different behavior of the energy spectrum and the influence of internal dynamic characteristics on it. Thus, in the works [29–32] the formation of sharp vorticity gradients in two-dimensional hydrodynamic turbulence and their influence on turbulent spectra due to flow anisotropy are considered. The energy accumulation on the scale of the system size leads to the emergence of intense large-scale motion, including large vortices [26]. The tendency towards the formation of

---

[1]Institute for Applied Mathematics, Far Eastern Branch, Russian Academy of Sciences, Vladivostok, Russian Federation
[2]Joint Institute for High Temperatures, Russian Academy of Sciences, Moscow, Russian Federation
[3]Institute for Computer Aided Design, Russian Academy of Sciences, Moscow, Russian Federation
[4]L.D. Landau Institute for Theoretical Physics, Russian Academy of Sciences, Chernogolovka, Russian Federation

large vortices has been indicated in the research devoted to two-dimensional turbulence, both experimental [47] and numerical [6, 9, 45, 46]. Large coherent vortices were observed in numerical simulation [10, 11, 42, 50] based on the solution of the two-dimensional Navier–Stokes equation with no-slip boundary condition. A similar coherent vortex structure was created in laboratory experiments in a square container [17, 49, 51]. Large vortices were obtained by numerical simulation of static pumping with various types of large-scale dissipation, as reported in [7, 48]. A whole series of computational works has been devoted to studying the properties of a coherent vortex [14, 25, 27, 33]. The first attempt to establish the profile of the average velocity of a coherent vortex was made in [33], where periodic boundary conditions and short-term time-correlated pumping were introduced. The authors show the appearance of a stable vortex dipole. In [25, 27], in a similar formulation, the average velocity profile of a coherent vortex was numerically found, which exhibits isotropy properties at a distance of the order of the vortex radius. Note that, in addition to Kolmogorov pumping, the presence of bottom friction has a significant effect on the formation of such flows, which is introduced into the system of equations under study by adding a term with a coefficient called the bottom friction coefficient [5].

In [14], Kolmogorov-type flow regimes in a square cell that occur at various values of the friction coefficient are numerically investigated. Three types of flow are most clearly classified: laminar, chaotic, and vortex flows. Transitional regimes arise between them, which are difficult to attribute to one type of flow [43], since they change their characteristics over time and are formed through a sequence of bifurcations during the change from a laminar flow to a chaotic flow regime, as well as during the transition from a chaotic to a vortex flow. In [13], the conditions for the existence of a vortex regime were identified and it was shown that it is observed at a sufficiently small value of the friction coefficient. The remaining flows occur when the coefficient is increased. However, this coefficient cannot be directly measured during a physical experiment in which the above flow regimes are observed. The measured characteristic for a two-dimensional flow during a physical experiment is the velocity field. Therefore, a natural problem arises to formulate an algorithm for processing the velocity field, which can be used to answer the question of what state (laminar, chaotic, vortex, or transitional) the hydrodynamic system is in. This will allow us to determine the value of the friction coefficient corresponding to a numerical experiment with the same parameters as in a physical experiment. In [21], for the first time, a method was proposed to classify structure on the analysis of rank distributions [22, 39] for the vorticity field and the frequency of occurrence of various values of this parameter. In [21], a differential characteristic of the vorticity distribution was revealed for various flow regimes of a viscous, slightly compressible fluid that occurs in a square region under the influence of a constantly acting force. This characteristic is determined by the coordinates of the inflection point for the rank distribution of the frequency of occurrence of vorticity. At the same time, numerical modeling has shown that there is no inflection point for the laminar regime; in the case of chaotic motion, it is formed, and when switching to the vortex flow regime, it shifts to the region of high ranks. Thus, the appearance of an inflection point can be used to analyze the types of flows. Since earlier [13, 14] flows were studied at various values of the pumping force and the bottom friction coefficient and a rank analysis was performed only for the vorticity field [21], it is necessary to perform a rank analysis of flow regimes for other characteristics of the model: energy and pressure, as well as to investigate the behavior of the corresponding inflection points of the rank curves. This paper presents a solution to this problem.

Let us briefly describe the content of the work. Section 1 presents a system of equations for the Kolmogorov-type flow and the results of a numerical experiment to identify the types of flows depending on the bottom friction coefficient. In Section 2, the general idea of constructing rank distributions for analyzing system properties is formulated. Sections 3, 4 and 5 are devoted to the analysis of the rank distributions of their values and the corresponding occurrence rates for vorticity, energy, and pressure. The appearance of an inflection point for the rank distributions of the frequency of occurrence of the studied characteristics is shown when the flow regimes change. The article ends with Discussion and Conclusion. For steady-state laminar flow, Appendix provides the construction of an analytical solution and the corresponding rank distribution, and a comparison with the results of numerical simulation is performed.

1. Model Relations and Calculation Results

We study the two-dimensional motion of a viscous weakly compressible fluid in a square cell Ω, satisfying the system of Navier–Stokes equations. The corresponding equations of continuity (1), momentum variation (2), (3), and weak compressibility (4) are presented below:

$$\frac{\partial \rho}{\partial t} + \nabla(\rho \bar{V}) = 0, \tag{1}$$

$$\frac{\partial \rho u}{\partial t} + \nabla(\rho u \bar{V}) = -\frac{\partial p}{\partial x} + \rho G \sin ky + \mu \Delta u - \zeta u, \tag{2}$$

$$\frac{\partial \rho v}{\partial t} + \nabla(\rho v \bar{V}) = -\frac{\partial p}{\partial y} - \rho G \sin kx + \mu \Delta v - \zeta v, \tag{3}$$

$$\mathrm{d}p = c^2 \rho_0 \frac{\mathrm{d}\rho}{\rho}. \tag{4}$$

Here ρ is the density of the liquid ($\rho_0 = 1000 \, \text{kg/m}^3$ is the initial density); $\bar{V} = (u, v)$ is the velocity vector, the components of which are equal, respectively, to u and v; $\mu = 0.1 \, \text{Pa} \cdot \text{s}$ is the dynamic viscosity of the liquid; p is pressure; ζ is the coefficient characterizing the presence of bottom friction; $G = 0.15 \, \text{m/s}^2$ is the amplitude of the external force; $k = 5 \, \text{m}^{-1}$ is the spatial frequency of the external force; c is the speed of the disturbance propagation. The right-hand sides of equations (2) and (3) contain the terms $\rho G \sin ky$ and $-\rho G \sin kx$, which model the action of the pumping force. The components $-\zeta u$ and $-\zeta v$ characterize the bottom friction force. For velocity, the no-slip condition is required at the boundary of the calculation cell: $\bar{V}|_{\partial \Omega} = 0$. The boundary condition for pressure is $\nabla_n p|_{\partial \Omega} = 0$, here $\partial \Omega$ is the outer boundary of the computational cell Ω, $\bar{n}$ is a vector perpendicular to the boundary surface.

The dimensionless parameter characterizing the formed flow regime is the Reynolds number $Re = \rho_0 V_{max} L / \mu$, here $L = 2\pi \, \text{m}$ is the size of the computational area, V_{max} is the maximum modulus of the flow velocity. The end time of the calculation was selected after the system reached a statistical stable state.

The initial conditions are undisturbed pressure and velocity fields: $P_0 = 10^5 \, \text{Pa}$, $u = v = 0 \, \text{m/s}$.

In equation (4) the speed of the disturbance propagation is $c = 100$ m/s. The choice of such a speed value allows us to achieve a compromise between the time step and the stability of the calculations. For the McCormack scheme, the following relationship between the time step, the space step, and other quantities has been empirically established [1], ensuring the stability of the scheme:

$$\Delta t \leq \frac{\sigma \Delta x}{\left(V_{max} + \sqrt{2}c\right)\left(1 + 2/Re_{min}\right)}, \qquad (5)$$

here σ is the safety factor, $\Delta x \approx 1.2 \cdot 10^{-2}$ m is the spatial step, $V_{max} \sim c/10$. Let us consider the case of a coarse computational grid, as the most favorable in terms of computational time. For laminar flow $Re = 900$ and we assume the minimum $Re_{min} \sim 200$, and we choose the coefficient σ equal to 1. Then from formula (5) it follows that $\Delta t \leq 8 \cdot 10^{-5}$ s. If $\sigma = 0.5$, then $\Delta t \leq 4 \cdot 10^{-5}$ s. For the calculations presented in this paper, a time step of $\Delta t = 2.5 \cdot 10^{-5}$ s was used.

The numerical solution of the Navier–Stokes equations is based on the artificial compressibility method [1]. In this case, the hyperbolic part of the equations is solved by the explicit McCormack method [37], whereas the parabolic part is solved by the standard finite difference method. The McCormack scheme has a second order of accuracy in space and time.

The McCormack scheme is used for the numerical solution of hyperbolic equations, since it has good dissipative and dispersion properties. In addition, it enables to study the behavior of quantities with large gradients, including discontinuities. To understand how suitable this numerical tool is for modeling turbulence, a test was performed, presented in [12, 15]. Overall, the McCormack scheme showed similar results to those that can be obtained using algorithms based on the CABARET scheme and the OpenFOAM finite volume method.

The numerical code is parallelized using the OpenMP library, designed for computers with shared memory. The calculations used the number of cores up to 384.

In [43], three main flow regimes were obtained: laminar, in which the fluid motion pattern retains its initial shape and does not change over time; chaotic (or turbulent), characterized by the presence of randomly moving vortices of various sizes and lifetimes; and vortex, in which a single large coherent vortex appears, it occupies almost the entire computational area and exists for a long time. In the course of a numerical experiment, the dependence of the flow type on the value of the bottom friction coefficient $\alpha = \zeta/\rho_0$ was analyzed. In order to identify it, numerical experiments were performed for various values of α and fixed values of G, μ. The dimensions of the parameters α, G, μ are equal to s^{-1}, m/s^2, Pa $\cdot$ s. It should also be emphasized that we did not set out the task of obtaining results that could be used as the basis for describing physical experiments on turbulence. Discussions with experimental scientists led us to the conclusion that at this stage of the numerical experiment it is necessary to develop a mathematical model that could qualitatively identify new effects of vortex motion. Therefore, the values of the simulation parameters, in particular, regarding viscosity, were selected based on the principle of "saving" computing resources. The experiments were carried out in the range for α from 10^{-4} to 1 and allowed us to identify the presence of transitional flow regimes occurring between the main regimes [43].

Figure 1 shows the vorticity fields of the forming flow depending on the value of α, all other simulation parameters are fixed. The value of the bottom friction coefficient $\alpha = 1$ corresponds to the stationary distribution of the velocity field determined by the pumping force. We call this laminar regime (Fig. 1a). When the coefficient α is in the range from 10^{-1} to $3 \cdot 10^{-1}$, a flow is formed (Fig. 1b) which is transitional from laminar to chaotic (Fig. 1c). This type of flow is characterized by the appearance of a system of vortices with positive and negative vorticity (Fig. 1b). Their position and shape have small deviations from the stationary distribution of the vorticity field. As the bottom friction coefficient decreases, the amplitude of vortex oscillations around their stationary position increases, as well as their size and shape change. The criterion
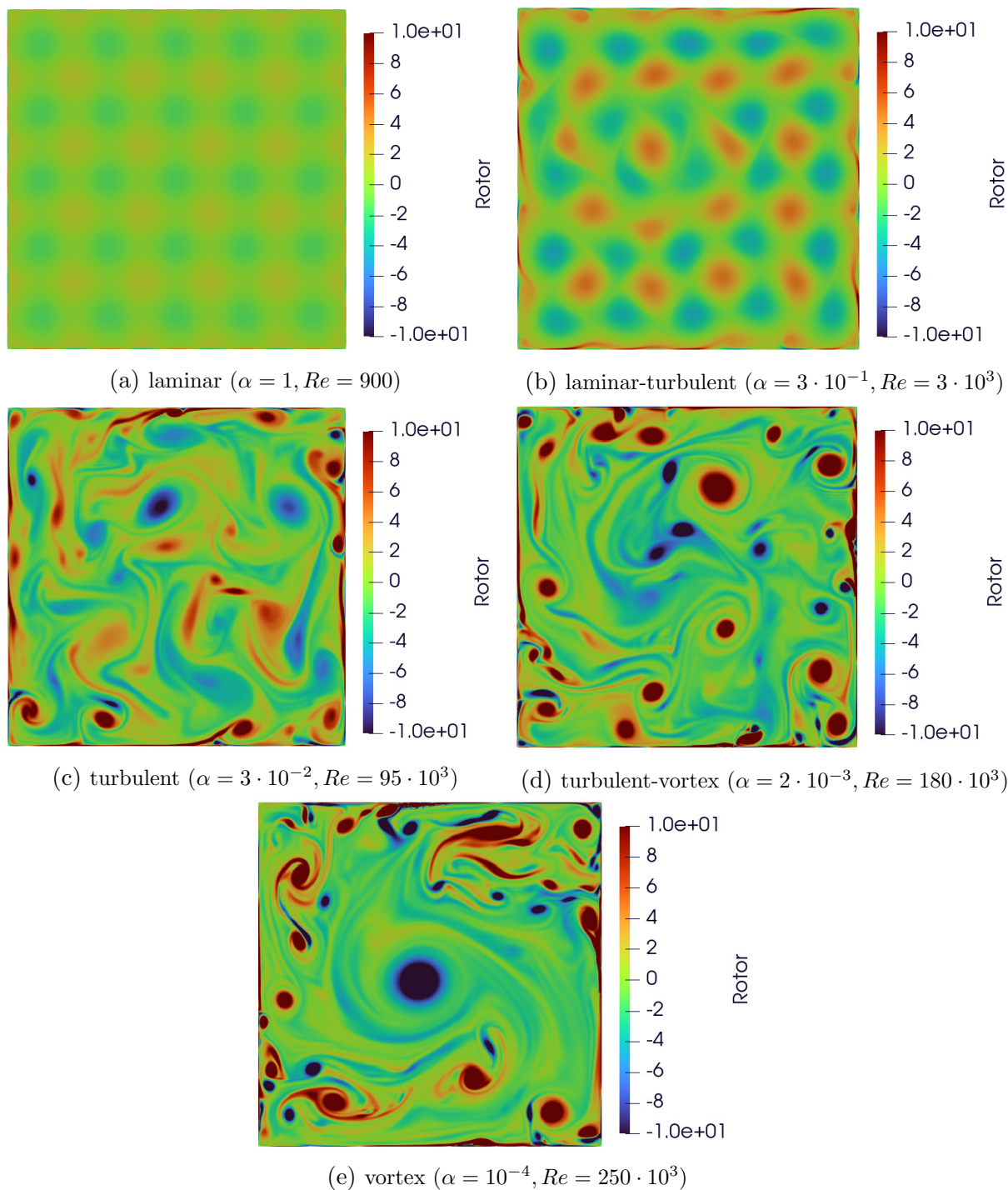
(a) laminar ($\alpha = 1, Re = 900$)

(b) laminar-turbulent ($\alpha = 3 \cdot 10^{-1}, Re = 3 \cdot 10^3$)

(c) turbulent ($\alpha = 3 \cdot 10^{-2}, Re = 95 \cdot 10^3$)

(d) turbulent-vortex ($\alpha = 2 \cdot 10^{-3}, Re = 180 \cdot 10^3$)

(e) vortex ($\alpha = 10^{-4}, Re = 250 \cdot 10^3$)

Figure 1. Vorticity fields with fixed parameters $G = 0.15$, $\mu = 0.1$,
and various α for different types of flow

for the transition to a chaotic regime (Fig. 1c) is the separation of vortices from their initial location and their chaotic movement around the cell. The chaotic flow in the figure corresponds to the value of the bottom friction coefficient in the range from $\alpha = 10^{-2}$ to $\alpha = 10^{-3}$. A decrease in the bottom friction coefficient to $\alpha = 10^{-4}$ leads to the appearance of a vortex regime (Fig. 1e), which is characterized by the formation of one large structure occupying the entire computational cell. Also, at the value of $\alpha = 2 \cdot 10^{-3}$, a regime transitional between the

chaotic and vortex ones is observed (Fig. 1d), which is characterized by the alternate existence of a chaotic flow and a coherent vortex.

2. A Method for Analyzing Flows according to Rank Distributions

As it is known, frequency-rank distributions have been used for a long time in various fields of human activity in describing quantitative characteristics of observed phenomena. The fact of their application was discovered in the first half of the twentieth century and is associated with works that have become classical in the field of demography [3], scientometrics [35], biology [18], seismology [20], linguistics [52], etc. It should be noted that, for frequency-rank distributions, foreign researchers [41] use the term "power-law distributions". In [8], the authors give a large number of examples from physics, earth sciences, biology, ecology, paleontology, computer and information sciences, and engineering and social sciences and show that they manifest a power-law distribution with the corresponding parameters. In the modern Russian literature devoted to the problem of rank distributions, we point out the paper [44], in which, as applied to ecology, modern surveys on rank distributions are discussed, and also the paper [36], which contains a rank analysis of technical systems.

Among the rank distributions, a special place is occupied by distributions described by the laws of Zipf, Pareto, Lotka, Mandelbrot, and others. Rank distributions involve the rank r (number) of an object and the frequency E of occurrence of the considered characteristics of the object: the rank is set and the frequency of occurrence is assigned to it. In particular, if, for some rather large text, one compiles a list of all words that occur in the text and then rank these words in decreasing order of the frequency E of their occurrence in the text, then, according to the Zipf's law [44], the multiplication of the rank r of a word and the frequency of occurrence E is constant: $rE = const$. Modifications of the Zipf's law were proposed for other rank distributions; however, there are sufficiently many phenomena for which the description of their characteristics is inconsistent with the above laws.

This stimulated researchers both to search for dependencies approximating empirical data more accurately and to formulate general models leading to rank distributions. In linguistics, when analyzing texts, Mandelbrot's model representations are known [38], in which he explains the Zipf's law using the concept of value of the optimal word code under the assumption that the text consists of words, separated by spaces, and is generated by some random process. A comparison of this approach with others is presented in the survey [34]. During the same decade, A.N. Kolmogorov, one of the founders of the probability theory, outlined in his works a way to revise the probability theory [24], from the viewpoint of the algorithmic approach. According to his approach, the notion of randomness was defined by him as the maximally complicated one. If one explains every random event in a deterministic way, then the algorithm for its occurrence will be very complex, and the decoding of this algorithm will require a very long code. The more complex the description of information, the longer is the required decryption algorithm, and this, according to Kolmogorov, is close to randomness.

A.N. Kolmogorov's concept obtained a constructive implementation in the works of V.P. Maslov, which enables us to study the behavior of observable characteristics without dividing them into deterministic and random ones. His approach differs essentially from that of Zipf, as well as from that of all other researchers who have studied this problem. Namely, he

used another representation in which the number of repeating values of a quantity is regarded as the observed quantity. Let us explain the general approach of V.P. Maslov [39, 40].

Let there be repeating values among the values x_i:

$$x_1 = x_2 = \ldots = x_{N_1}, x_{N_1+1} = x_{N_1+2} = \ldots = x_{N_2}, \ldots, x_{N_{k-2}+1} = x_{N_{k-2}+2} = \ldots = x_{N_{k-1}}$$

$$x_{N_{k-1}+1} = x_{N_{k-1}+2} = \ldots = x_{N_k}, \sum_{i=1}^{k} N_i = N,$$

i.e., the family of numbers $N_1, N_2, \ldots, N_k$ specifies how many times the values $x_{N_1}, x_{N_2}, \ldots, x_{N_k}$ are repeated. Let n_i, $i = 1, \ldots, p$, denote the number of x_i with the same frequency of their occurrence E_i,

$$N_1 = \ldots = N_{n_1} \equiv E_1, N_{n_1+1} = \ldots = N_{n_2} \equiv E_2, \ldots, N_{n_{p-2}+1} = \ldots = N_{n_{p-1}} \equiv E_{p-1},$$

$$N_{n_{p-1}+1} = \ldots = N_{n_p} \equiv E_p,$$

and the values E_i are ordered, i.e., $0 \leq E_i \leq E_{i+1}$. According to the terminology adopted in linguistics, the frequencies of occurrence E_i form a dictionary [40], and n_i is the number of words with the same frequency of occurrence. In this consideration, the frequency E_i acts as an observable value and the number of values n_i with this frequency characterizes the number of realized values E_i. With fairly general assumptions, V.P. Maslov proposed a formula relating the rank r_s of the s-th word to frequency:

$$r_s = \sum_{i=1}^{s} \frac{1}{\exp(\beta E_i + \sigma) - 1}. \tag{6}$$

Here, the parameters β and σ are given by the normalization conditions (the exact formulation of this assertion in the form of a theorem is given in [39]). Thus, formula (6) implements an algorithm of deterministic calculation of the cumulative probability. In this consideration, the frequency E_i acts as a random variable, and the number n_i of words with this frequency characterizes the number of occurrences of this random variable. This distinguishes Maslov's consideration from the approach adopted in linguistic statistics. The idea of using a new kinematic set of variables in the study of the behavior of the observed characteristics of the system was earlier constructively implemented in the work of V.A. Fock on the secondary quantization method [16]. This method was used to construct a wave function when describing a system of quantum particles. According to Fock's idea, it is convenient to analyze the equation for this function not in the configuration space, but in the space of occupation numbers or, in the terminology of quantum mechanics, in the Fock space. In other words, to describe the system, one should select a set of variables to which Fock has moved using the canonical transformation.

In fact V.P. Maslov proposed a representation in which frequency is considered as an observable, and the number of values of the initial variable with this frequency characterizes the number of realized frequency values. With this approach, the Maslov frequency is similar to the Fock's canonically conjugate variable (energy), and the number of realized frequency values corresponds to the number of occupation.

In [21] we constructed an algorithm for classifying Kolmogorov-type flows using the knowledge about their velocity field. The main difficulty in analyzing the characteristics of a chosen dynamical system was the formation of information that is suitable for creating a corresponding algorithmization procedure. We used the theoretical concepts of V.P. Maslov that suggest an

interpretation of the information data as a semiotic system in which the values of the vorticity of the velocity field are regarded as signs [21]. The rank analysis was performed first for specific values of vorticity, which enables us to obtain its distribution. Then, the rank curves were constructed for the frequency of the vorticity recurrence, which correspond to the flow regime as a whole. To obtain the functional dependence of rank on frequency based on formula (6), we used the parameterization for the frequency of occurrence proposed by V.P. Maslov. It was shown that it is possible to identify different fluid motion regimes for Kolmogorov-type flows by comparing them with the graphs of the rank distributions of the vorticity.

Since it was assumed that, in the process of evolution of the system, some forms of order are created in it, it follows that, from the point of view of semiotics, the patterns in the distribution of different signs should occur. Therefore, we will consider the values of energy and pressure as an additional set of signs for which we construct rank distributions of their values and frequencies of their occurrence. It is shown that the rank curves of the vorticity, energy, and pressure fields and their frequencies are divided depending on the type of flow. This behavior can be used to identify and analyze different flow patterns. When conducting a rank analysis, the curves obtained make it possible to establish an unambiguous relationship between behavior a graph of the rank curve and the corresponding type of flow.

The construction of a rank distribution for a parameter X of an arbitrary physical system can be performed in two ways. The value of X is considered for 100 time steps starting from 700th iteration, which corresponds to reaching a statistical stationary state. For each moment in time, the value of X is calculated in each cell of the computational domain. After that, the values of X obtained for all moments in time are combined into one data array. It is sorted in ascending order of the value of X, and each value is assigned a serial number (rank). The rank is understood as the ordinal number in the ascending (or descending) sequence of values of X.

When using the second method, we move in the description of the system from the variable X to the frequency E of occurrence of this variable. The values of E are sorted from lower to higher, and for the resulting array of values, a distribution is constructed for E depending on the rank r. The implementation of the first approach does not lead to any difficulties. In the algorithmic implementation of the second approach, we identify the minimum $X_{\min}$ and maximum values of $X_{\max}$ of the variable X in the computational domain. Setting $\Delta = (X_{\max} - X_{\min})/N$, where N is the number of intervals selected a priori (in what follows, $N = 100$), we subdivide the segment $[X_{\min}, X_{\max}]$ into intervals of length Δ. In this case, the calculated values of X_k fall within one of these intervals. Calculating the number of values of X_k that fall within one of the intervals, we obtain the frequency E_k of occurrence of the parameter X. As a result, we have an array of length N containing the frequency of occurrence E_k. Finally, this array is sorted: the largest value of the frequency of occurrence E_k is assigned the largest ordinal number (rank) of r, and the smallest value of E_k is assigned the smallest rank of r. Note that traditionally, when considering chaotic flows, a single-point probability density function (PDF) is used. PDF vorticity distributions were constructed for laminar, turbulent, and vortex flow regimes. For the same regimes, rank dependencies of the vorticity frequency of occurrence were constructed [21]. Both in case of rank analysis and in case of constructing a PDF distribution, the same values of the vorticity frequency of occurrence are used. The difference between these approaches lies in different data processing: when performing rank analysis, the frequency of occurrence is distributed depending on the rank, and in case of PDF analysis, the frequency of occurrence is distributed depending on the value of vorticity.

3. Rank Analysis of Vorticity

In accordance with the idea proposed above, we will perform the construction of rank curves for the vorticity value using the rank analysis methodology described in Section 2. Figure 2a shows the vorticity distribution for different bottom friction coefficients. Note the characteristic behavior of the plotted graphs. The curves corresponding to different flow regimes are arranged in a certain sequence. This is clearly seen in the graph for negative vorticity (Fig. 2a). The graph corresponding to the laminar regime can be approximated by a linear function, for which the bottom friction coefficient α is 1. In Appendix, an analytical solution has been built for this regime. As α decreases to 10^{-1}, the shape of the rank distribution graph changes, and the curvature of the graph increases in the area of higher ranks. This corresponds to a regime change from laminar to chaotic. Various forms of turbulent flows are observed in the range of the bottom friction coefficient from 10^{-1} to 10^{-3}. When α changes from 10^{-3} to 10^{-4}, a large coherent vortex formation regime is realized. Separately, it is worth noting that due to the averaging of 100 output over time, the total number of ranks with this approach is about 10^7.

Figure 2b shows the vorticity frequency of occurrence E graphs for various flow regimes. The laminar and vortex regimes correspond to convex functions with different asymptotic behavior. Note that the rank distribution graphs for the turbulent regime have a characteristic S-shape. Analysis of the rank distribution curves for the vorticity frequency of occurrence reveals the presence of an inflection point on the graph. The red dots in Fig. 2b indicate the inflection points.
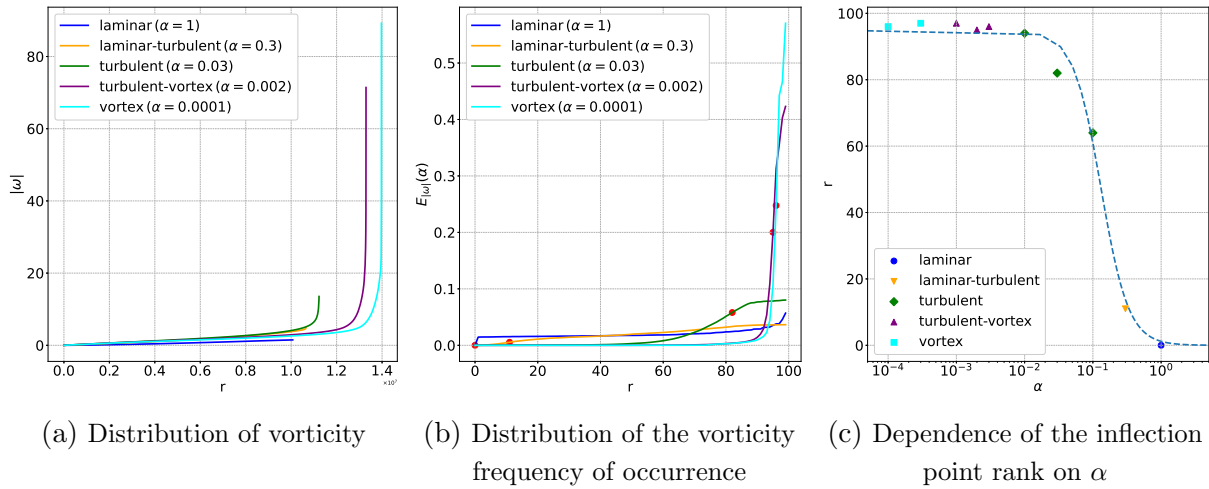

(a) Distribution of vorticity

(b) Distribution of the vorticity frequency of occurrence

(c) Dependence of the inflection point rank on α

Figure 2. Rank analysis of vorticity for different type of flows

Thus, considering the entire range of the bottom friction coefficient α, the following properties of the constructed distributions can be distinguished. First, when the flow regimes change, the inflection point appears in the graphs of the corresponding rank distributions. Secondly, for each type of flow, this inflection point has its own rank. The dependence of the inflection point rank on α on a logarithmic scale is shown in Fig. 2c. The gray triangles in this graph correspond to the vortex regime, which is characterized by high inflection point ranks and low values of the bottom friction coefficient (the range of α is from 10^{-3} to 10^{-4}). For the laminar regime, the inflection point has small ranks, which correspond to the orange triangles on the graph (the range of α is from 1 to 10^{-1}). For this regime, an analytical solution is constructed in Appendix, for which the frequency distributions of vorticity are indicated. Comparison of

them with numerical results shows a satisfactory correspondence between them. The turbulent type of flow occurring in the range of α from 10^{-1} to 10^{-3} has a wide range of rank values for the inflection point, ranging from large to small. The dependence of the rank of the inflection point on the friction coefficient α can be approximated using the relation:

$$r = \frac{A}{1 + B(\alpha/\alpha_0)^\gamma}. \tag{7}$$

Here α_0 is the dimensional coefficient equal to $1\,\mathrm{s}^{-1}$; A, B and γ are the fitting parameters corresponding to the values 95, 78 and 2.1 for this graph.

4. Energy Rank Analysis

Let us consider another parameter of the flow, energy, and perform a rank analysis for it. Figure 3a shows the energy distribution for different bottom friction coefficients. Note the characteristic behavior of the plotted graphs. The curves corresponding to different flow regimes are arranged in a certain sequence. This is clearly seen in Fig. 3a. The graph corresponding to the laminar regime can be approximated by a linear function, for which the bottom friction coefficient is $\alpha = 1$. As α decreases to 10^{-1}, the shape of the rank distribution graph changes, the curvature of the curve changes in the area of high ranks, and the energy value increases. This corresponds to a regime change from laminar to chaotic. In the range of changes in the bottom friction coefficient from 10^{-1} to 10^{-3}, various forms of turbulent flows and a further increase in energy in the range of higher grades are observed. When α changes from 10^{-3} to 10^{-4}, a large coherent vortex regime is realized. The energy reaches its maximum value for this regime. The localization of the energy on the macroscopic scale of pumping corresponds to the formation of the Kraichnan reverse energy cascade [28] for this system. It is worth noting separately that due to averaging over 100 issues over time, the total number of ranks with this approach is approximately $1.8 \cdot 10^7$. There are more of them than in the vorticity analysis, since only negative vorticity was used for consideration.

The results of the rank analysis of the energy frequency of occurrence for different flow regimes are shown in Fig. 3b. The convex functions of the rank distribution with different asymptotic behaviors correspond to the laminar and vortex regimes. Note that the rank distribution graphs for the turbulent regime have a characteristic S-shape. Analysis of the rank distribution curves of the energy frequency of occurrence, as in case of vorticity, reveals the presence of an inflection point on the graph. The red dots in Fig. 3b indicate the inflection points. In the region of high ranks, localization of curves corresponding to laminar, chaotic, and vortex regimes is noticeable. In particular, for laminar regime, the frequency of occurrence of energy depends almost linearly on the rank and its value does not exceed 0.02. An increase in the frequency of energy occurrence to 0.09 for the ranks in the range from 80 to 100 corresponds to the turbulent regime. For the vortex regime, there is a sharp increase in the frequency of occurrence to 0.14, starting from a rank equal to 95.

Considering the entire range of the bottom friction coefficient α, we can again identify two characteristic properties of rank distributions. Firstly, when the flow regimes change, an inflection point appears on the corresponding graphs. Secondly, for each type of flow, the inflection point has its own rank and its dependence on α is shown in Fig. 3c. For vortex and turbulent regime, the position of the inflection point is localized in the region of high ranks. In the course of transition from a chaotic regime to a laminar one, corresponding to the range of the
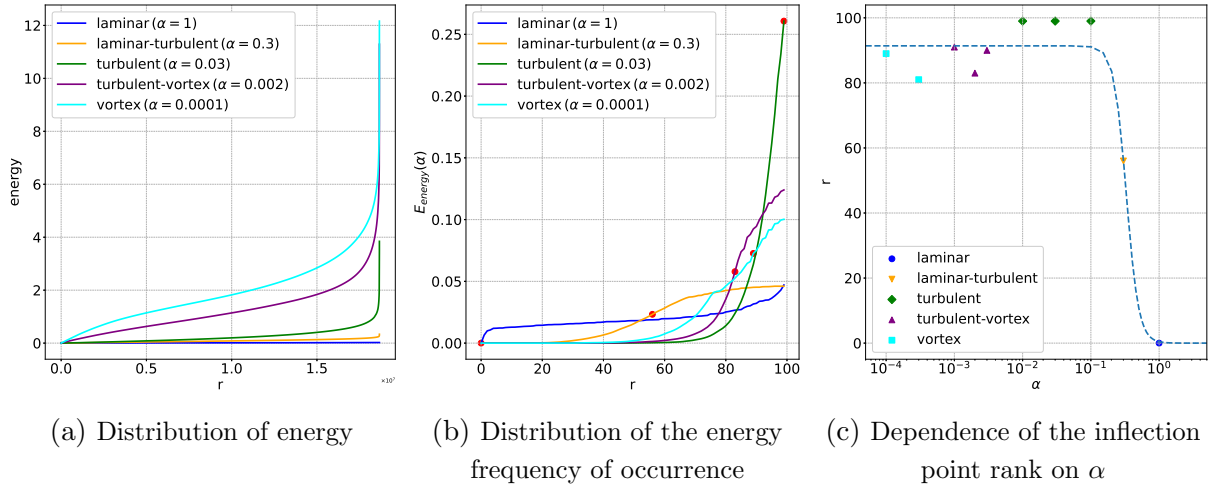
(a) Distribution of energy

(b) Distribution of the energy frequency of occurrence

(c) Dependence of the inflection point rank on α

Figure 3. Rank analysis of energy for different type of flows

bottom friction coefficient from 10^{-1} to 1, there is a sharp change in the rank of the inflection point to the minimum values. The graph of the dependence of the inflection point rank on the bottom friction coefficient can also be approximated by dependence (7) with coefficients $A \sim 91$, $B \sim 200$, $\gamma \sim 4.8$.

5. Pressure Rank Analysis

Figure 4a shows the pressure distribution for various coefficients α. Note that the graph in Fig. 4a has partial symmetry with respect to the horizontal straight line corresponding to the initial pressure distribution. For the laminar regime, localization of the rank curves relative to this distribution is observed. The transition to turbulent and vortex regime leads to a change in density and, as a result, a deviation (negative for small ranks and positive for large ranks) of the pressure value. The localization of curves corresponding to laminar, chaotic, and vortex regime is noticeable. The total number of ranks, similar to the previous paragraph, is about $1.8 \cdot 10^7$.

For the laminar regime, localization of the rank curves relative to this is observed. For laminar regime, its value does not exceed 0.5 percent of the initial distribution. In turbulent regime, there corresponds an increase in pressure deviations of up to 5 percent. For the vortex regime, there is a sharp increase in pressure deviations of up to 15 percent. Let us now consider the results of a rank analysis of the pressure frequency of occurrence for various flow regimes (Fig. 4b). Convex functions of rank distributions with different asymptotic behavior correspond to the laminar and vortex regimes. For the turbulent regime, a characteristic S-shaped pattern is realized for the rank distribution graphs. Analysis of the rank distribution curves for pressure frequency, as in case of vorticity and energy, reveals the presence of an inflection point on the graph.

Thus, considering the entire range of changes in the value of the friction coefficient α, we observe the appearance of an inflection point on the graphs of the corresponding rank distributions, while for each type of flow the inflection point has its own rank. The red dots in Fig. 4b indicate the inflection points. The dependence of the inflection point rank on α is shown in Fig. 4c. For vortex and turbulent regimes, the value of this rank is localized in the region of its high values. When switching from a chaotic regime to a laminar one, corresponding to the

range of the bottom friction coefficient from 10^{-1} to 1, there is a sharp change in the rank of the inflection point to the minimum values.

(a) Distribution of pressure   (b) Distribution of the pressure frequency of occurrence   (c) Dependence of the inflection point rank on α
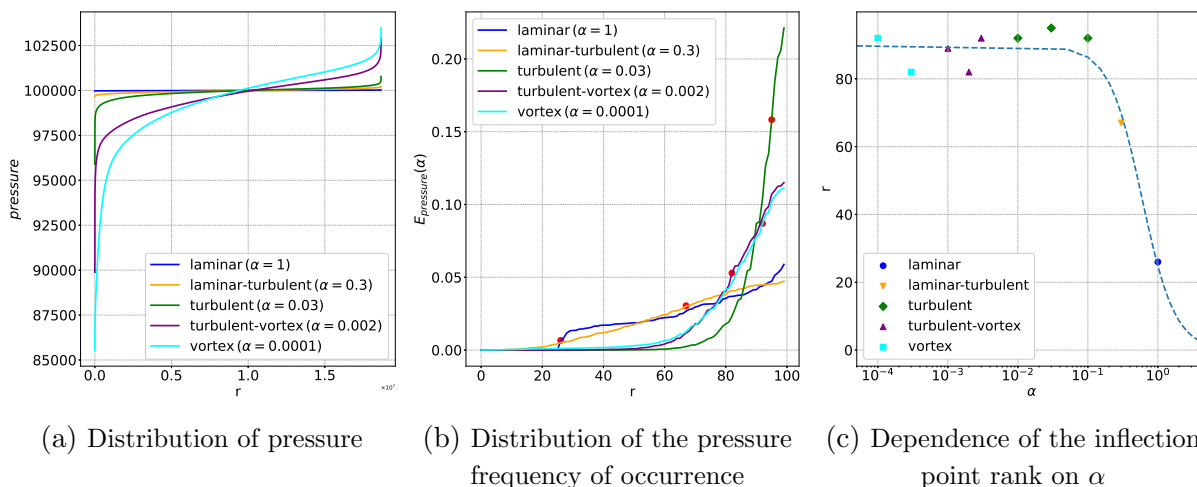
Figure 4. Rank analysis of pressure for different type of flows

The graph of the dependence of the inflection point rank on the bottom friction coefficient can also be approximated by the dependence (7) with coefficients $A \sim 90$, $B \sim 2.6$, $\gamma \sim 1.8$.

Discussion

Earlier, the problem of analyzing the rank distributions for vorticity, energy, and pressure was formulated. The calculation results obtained in this paper demonstrate that the constructed rank curves for these quantities have similar behavior. It consists in the fact that for laminar flows, the behavior of the corresponding quantities, depending on the rank, is approximated by a linear function. When the flow regimes change, the graphs become significantly nonlinear in the area of high ranks. The analysis of the rank distribution of the frequency of occurrence for vorticity, energy, and pressure showed that when the flow regime changes, an inflection point appears for the graphs of all the indicated of the frequency of occurrence. Thus, the appearance of an inflection point can be used to analyze the types of fluid motion. The dependence of the inflection point rank on the bottom friction coefficient, which is responsible for changing the flow regime in the numerical experiment, makes it possible to establish a relationship between the internal parameter, the bottom friction coefficient and the velocity field observed in the physical experiment.

Conclusion

The problem of two-dimensional flow of a viscous fluid in a square cell under the influence of an external force (Kolmogorov-type flow) and the presence of bottom friction is considered. The analysis of the emerging flow types during the transition from the laminar flow type to the vortex flow occurs through a series of bifurcations, including the turbulent flow type. The use of rank distributions in analyzing the obtained flows allows us to look at vortex hydrodynamic processes from a new perspective and supplement the characteristics of flow regimes with such parameters as the inflection point of the frequency of vorticity, energy and pressure. This method makes it possible to determine how the rank curves for vorticity, energy, and pressure fields and their

frequencies are divided according to the flow type, which can be further used for identifying and analyzing various flow regimes. When performing a rank analysis, the obtained curves allow us to establish an unambiguous relationship between the behavior of the graph of the rank curve and the corresponding type of flow. Thus, the proposed approach makes it possible to classify flow regimes according to a given velocity field.

In our work, we consider the general idea of rank analysis for a system with a spatiotemporal internal structure, that is, endowed with some forms of order. It has been shown numerically that for the Kolmogorov problem, laminar, turbulent, and vortex flow regimes appear for each fixed value of the driving force, depending on the values of the bottom friction coefficient. In case of each of the structures, the rank distributions of the observed values were constructed and a comparison was made to the selected flow regime, which in a sense is characteristic of this system distribution.

Appendix

The laminar (stationary) solution in the linear approximation satisfies the equations

$$-\frac{\partial p}{\partial x} + \rho G \sin ky + \mu \Delta u - \zeta u = 0, \quad -\frac{\partial p}{\partial y} - \rho G \sin kx + \mu \Delta v - \zeta v = 0. \tag{8}$$

The vorticity is equal to

$$\omega = \frac{\partial v}{\partial x} - \frac{\partial u}{\partial y}.$$

Assuming $\rho = const$, we obtain from (8) the following equation for vorticity:

$$-\mu \Delta \omega + \zeta \omega + \rho G k [\cos kx + \cos ky] = 0.$$

The solution for ω is given by the formula

$$\omega = \frac{\rho G k}{\zeta + k^2 \mu} [\cos kx + \cos ky].$$

The graph (Fig. 5) shows the frequency distributions of negative vorticity, obtained numerically (blue line) and analytically (red dotted line).
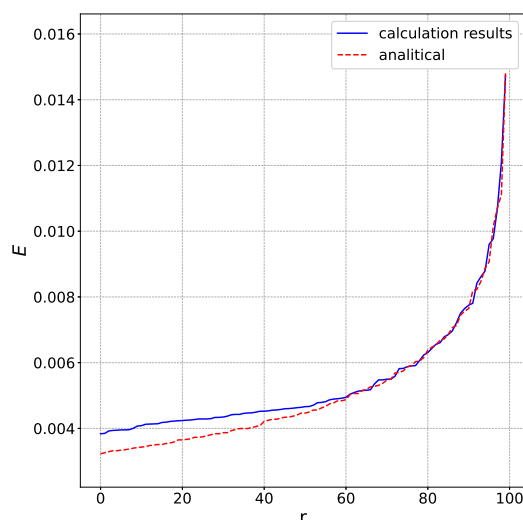
Acknowledgements

Figure 5. Rank distribution for negative vorticity for the laminar flow regime, constructed analytically and numerically

References

1. Anderson, D.A., Tannehill, J.C., Pletcher, R.H.: Computational Fluid Mechanics and Heat Transfer. Taylor and Francis (2016). `https://doi.org/10.1201/b12884`

2. Arnold, V.I., Meshalkin, L.D.: A. N. Kolmogorov's seminar on selected issues of analysis (1958-1959). Russ. Math. Surv. 15, 247–250 (1960)

3. Auerbach, F.: Das Gesetz der Bevölkerungskonzentration. Petermanns Geographische Mitteilungen 59, 74–76 (1913)

4. Batchelor, G.K.: Computation of the Energy Spectrum in Homogeneous Two-Dimensional Turbulence. Phys. Fluids 12, 233–239 (1969). `https://doi.org/10.1063/1.1692443`

5. Bondarenko, N.F., Gak, M.Z., Dolzhansky, F.V.: Laboratory and theoretical models of plane periodic flow. Izvestiia, Fizika Atmosfery i Okeana 15, 1017–1026 (1979)

6. Borue, V.: Inverse energy cascade in stationary two-dimensional homogeneous turbulence. Phys. Rev. Lett. 72, 1475 (1994). `https://doi.org/10.1103/PhysRevLett.72.1475`

7. Chertkov, M., Connaughton, C., Kolokolov, I., Lebedev, V.: Dynamics of Energy Condensation in Two-Dimensional Turbulence. Phys. Rev. Lett. 99 (2007). `https://doi.org/10.1103/PhysRevLett.99.084501`

8. Clauset, A., Shalizi, C.R., Newman, M.E.J.: Power-Law Distributions in Empirical Data. SIAM Review 51(4), 661–703 (2009). `https://doi.org/10.1137/070710111`

9. Clercx, H.J.H.: A Spectral Solver for the Navier-Stokes Equations in the Velocity-Vorticity Formulation for Flows with Two Nonperiodic Directions. J. Comp. Phys. 137, 186–211 (1997). `https://doi.org/10.1006/jcph.1997.5799`

10. Clercx, H.J.H., Maassen, S.R., van Heijst, G.J.F.: Spontaneous spin-up during the decay of 2D turbulence in a square container with rigid boundaries. Phys. Rev. Lett. 80, 5129 (1998). `https://doi.org/10.1103/PhysRevLett.80.5129`

11. Clercx, H.J.H., Nielsen, A.H., Torres, D.J., Coutsias, E.A.: Two-dimensional turbulence in square and circular domains with no-slip walls. Eur. J. Mech. B-Fluids 20, 557–576 (2001). https://doi.org/10.1016/S0997-7546(01)01130-X

12. Denisenko, V.V., Doludenko, A.N., Fortova, S.V., *et al.*: Numerical modelling of the Kolmogorov flow in a viscous media, forced by the periodic on space static force. Computer Research and Modeling 14(4), 741–753 (2022). https://doi.org/10.20537/2076-7633-2022-14-4-741-753

13. Doludenko, A.N., Fortova, S.V., Kolokolov, I.V., Lebedev, V.V.: Coherent vortex in a spatially restricted two-dimensional turbulent flow in absence of bottom friction. Physics of Fluids 33, 1–6 (2021). https://doi.org/10.1063/5.0038863

14. Doludenko, A.N., Fortova, S.V., Kolokolov, I.V., Lebedev, V.V.: Coherent vortex versus chaotic state in two-dimension turbulence. Annals of Physics 447 (2022). https://doi.org/10.1016/j.aop.2022.169072

15. Doludenko, A.N., Kulikov, Y.M., Savel'ev, A.S.: Chaotic flow under the influence of volumetric force. Computer Research and Modeling 16(4), 883–912 (2024). https://doi.org/10.20537/2076-7633-2024-16-4-883-912

16. Fock, V.A.: Konfigurationsraum und zweite Quantelung. Zeitschrift für Physik 75, 622–647 (1932). https://doi.org/10.1007/BF01344458

17. Francois, N., Xia, Y., Punzmann, H., *et al.*: Three-Dimensional Fluid Motion in Faraday Waves: Creation of Vorticity and Generation of Two-Dimensional Turbulence. Phys. Rev. X 4 (2014). https://doi.org/10.1103/PhysRevX.4.021021

18. Gleason, H.A.: The Significance of Raunkiaer's Law of Frequency. Ecology 10(4), 406–408 (1929). https://doi.org/10.2307/1931149

19. Golitsyn, G.S.: A. N. Kolmogorov's 1934 paper is the basis for explaining the statistics of natural phenomena of the macrocosm. Physics-Uspekhi 67, 80–90 (2024). https://doi.org/2023.05.039355

20. Gutenberg, B., Richter, C.F.: Frequency of earthquakes in California. Bulletin of the Seismological Society of America 34(4), 185–188 (1944). https://doi.org/10.1785/BSSA0340040185

21. Guzev, M.A., Fortova, S.V., Doludenko, A.N., *et al.*: Maslov Rank Distributions for the Analysis of Two-Dimensional and Quasi-Two-Dimensional Turbulent Flows. Russian Journal of Mathematical Physics 31, 438–449 (2024). https://doi.org/10.1134/S1061920824030075

22. Guzev, M.A., Nikitina, E.Y., Chernysh, E.V.: V. P. Maslov's Approach to the Analysis of Rank Distributions. Russian Journal of Mathematical Physics 28, 56–65 (2021). https://doi.org/10.1134/S1061920821010064

23. Kolmogorov, A.N.: Doklady Akademii Nauk SSSR 30, 299–303 (1941)

24. Kolmogorov, A.N.: Three approaches to the definition of the concept "quantity of information". Probl. Peredachi Inf. 1, 3–11 (1965)

25. Kolokolov, I.V., Lebedev, V.V.: Structure of coherent vortices generated by the inverse cascade of two-dimensional turbulence in a finite box. Phys. Rev. E 93 (2016). `https://doi.org/10.1103/PhysRevE.93.033104`

26. Kolokolov, I.V., Lebedev, V.V.: Large-scale flow in two-dimensional turbulence at static pumping. JETP Lett. 106, 659–661 (2017). `https://doi.org/10.1134/S0021364017220027`

27. Kolokolov, I.V., Lebedev, V.V.: Coherent vortex in two-dimensional turbulence: Interplay of viscosity and bottom friction. Phys. Rev. E 102 (2020). `https://doi.org/10.1103/PhysRevE.102.023108`

28. Kraichnan, R.H.: Inertial Ranges in Two-Dimensional Turbulence. Phys. Fluids 10, 1417–1423 (1967). `https://doi.org/10.1063/1.1762301`

29. Kudryavtsev, A.N., Kuznetsov, E.A., Sereshchenko, E.V.: Statistical properties of freely decaying two-dimensional hydrodynamic turbulence. JETP Letters 96, 699–705 (2013). `https://doi.org/10.1134/S0021364012230105`

30. Kuznetsov, E.A., Naulin, V., Nielsen, A.H., Rasmussen, J.J.: Effects of sharp vorticity gradients in two-dimensional hydrodynamic turbulence. Physics of Fluids 19(10), 10 (2007). `https://doi.org/10.1063/1.2793150`

31. Kuznetsov, E.A., Naulin, V., Nielsen, A.H., Rasmussen, J.J.: Sharp vorticity gradients in two-dimensional turbulence and the energy spectrum. Theoretical and Computational Fluid Dynamics 24, 253–258 (2010). `https://doi.org/10.1007/s00162-009-0135-4`

32. Kuznetsov, E.A., Sereshchenko, E.V.: Anisotropic characteristics of the kraichnan direct cascade in two-dimensional hydrodynamic turbulence. JETP Letters 102(11), 760–765 (2015). `https://doi.org/10.1134/S0021364015230083`

33. Laurie, J., Boffetta, G., Falkovich, G., *et al.*: Universal Profile of the Vortex Condensate in Two-Dimensional Turbulence. Phys. Rev. Lett. 113 (2014). `https://doi.org/10.1103/PhysRevLett.113.254503`

34. Lees, R.B.: Logique, langage et théorie de l'information by Léo Apostel, Benoit Mandelbrot, Albert Morf. Language 35(2) (1959). `https://doi.org/10.2307/410536`

35. Lotka, A.J.: The Frequency Distribution of Scientific Productivity. Journal of the Washington Academy of Sciences 16(12), 317–323 (1926)

36. Lutsenko, D.V.: Combinatorial Theory of Rank Dynamics. Kaliningrad: Tekhnotsenoz (2018)

37. MacCormack, R.W.: A Numerical Method for Solving the Equations of Compressible Viscous Flow. AIAA Journal 20, 1275–1281 (1982). `https://doi.org/10.2514/6.1981-110`

38. Mandelbrot, B.: Statistical Macro-Linguistics. Il Nuovo Cimento (1955-1965) 13, 518–520 (1959). `https://doi.org/10.1007/bf02724682`

39. Maslov, V.P.: On one general theorem of set theory leading to the Gibbs, Bose-Einstein, Pareto distribution and the Mandelbrot–Zipf law for the stock market. Mat. notes. 78, 807–813 (2005). `https://doi.org/10.1007/s11006-005-0186-9`

40. Maslov, V.P.: Quantum Linguistic Statistics. Russian Journal of Mathematical Physics 13, 315–325 (2006). `https://doi.org/10.1134/S1061920806030071`

41. Mitzenmacher, M.: A Brief History of Generative Models for Power Law and Lognormal Distributions. Internet Mathematics 1(2), 226–251 (2004). `https://doi.org/10.1080/15427951.2004.10129088`

42. Molenaar, D., Clercx, H.J.H., van Heijst, G.J.F.: Angular momentum of forced 2D turbulence in a square no-slip domain. Physica D 196, 329–340 (2004). `https://doi.org/10.1016/j.physd.2004.06.001`

43. Posudnevskaya, A.O., Fortova, S.V., Doludenko, A.N., *et al.*: Numerical Study of Transient Regimes of Kolmogorov Flow in a Square Cell. Computational Mathematics and Mathematical Physics 64, 2102–2110 (2024). `https://doi.org/10.1134/S0965542524701033`

44. Puzachenko, Y.G.: Rank distribution in ecology and nonextensive statistical mechanism. Archives of Zoological Museum of Lomonosov Moscow State University 54, 42–71 (2016)

45. Smith, L.M., Yakhot, V.: Bose condensation and small-scale structure generation in a random force driven 2D turbulence. Phys. Rev. Lett. 171, 352 (1993). `https://doi.org/10.1103/PhysRevLett.71.352`

46. Smith, L.M., Yakhot, V.: Finite-size effects in forced two-dimensional turbulence. J. Fluid Mech. 274, 115–138 (1994). `https://doi.org/10.1017/S0022112094002065`

47. Sommeria, J.: Experimental study of the two-dimensional inverse energy cascade in a square box. J. Fluid Mech 170, 139–168 (1986). `https://doi.org/10.1017/S0022112086000836`

48. Tsang, Y.K.: Nonuniversal velocity probability densities in two-dimensional turbulence: The effect of large-scale dissipation. Phys. Fluids 22 (2010). `https://doi.org/10.1063/1.3504377`

49. Tsang, Y.K., R.Young, W.: Forced-dissipative two-dimensional turbulence: A scaling regime controlled by drag. Phys. Rev. E 79 (2009). `https://doi.org/10.1103/PhysRevE.79.045308`

50. Xia, H., Punzmann, H., Falkovich, G., Shats, M.G.: Turbulence-Condensate Interaction in Two Dimensions. Phys. Rev. Lett. 101 (2008). `https://doi.org/10.1103/PhysRevLett.101.194504`

51. Xia, H., Shats, M., Falkovich, G.: Spectrally condensed turbulence in thin layers. Phys. Fluids 21 (2009). `https://doi.org/10.1063/1.3275861`

52. Zipf, G.K.: Human behavior and the principle of least effort. Addison-Wesley Press (1949)